SIR Epidemic Model under Mobility on Multi-layer Networks ⋆

Vishal Abhishek * **and Vaibhav Srivastava** **

* *Department of Mechanical Engineering, Michigan State University, East Lansing, MI 48824-1226, USA (e-mail: abhishe3@msu.edu).*
** *Electrical and Computer Engineering, Michigan State University, East Lansing, MI 48824-1226, USA (e-mail: vaibhav@egr.msu.edu)*

Abstract: We study Susceptible-Infected-Recovered (SIR) epidemic model under mobility on multi-layer networks. We consider a scenario in which each individual within the population belong to one of the multiple classes and the population is distributed over multiple environmental patches. Individuals within a patch interact according to the SIR epidemic model and move across patches according to a class-dependent continuous time Markov chain. This yields a multi-layer network in which each layer is associated with a class and the connectivity in each layer corresponds to the digraph and transition rates of the associated Markov chain. For this multi-layer SIR model, we establish stability properties of equilibria using Lyapunov techniques, and derive simple conditions for the epidemic outbreak.

Keywords: Nonlinear analysis, Graph theoretic models, Dynamic modeling, Epidemic modeling, SIR model, Patchy environments

1. INTRODUCTION

The classic SIR epidemic model has been applied to several infectious diseases including smallpox, polio, measles, rubella, chickenpox, and influenza (Hethcote, 2000). Variations of the classic SIR model have also been used for predicting and designing mitigation strategies for the novel Coronavirus disease (Calafiore et al., 2020; Franco, 2020; Morris et al., 2020). Within the context of engineered systems, these models have been used to understand the spread of computer viruses (Kleinberg, 2007; Wang et al., 2009), routing in mobile communication networks (Zhang et al., 2007), and spread of rumors (Jin et al., 2013).

In this paper we focus on an environment comprised of multiple spatially distributed regions (patches) and study a model in which individuals within each patch interact with each other according to the SIR model and move across different patches according to a Continuous Time Markov Chain (CTMC). Individuals are clustered into classes and their mobility depends on the class. In the context of disease modeling, such mobility represents movement of individuals across highly populated neighborhoods, and different classes may correspond to age groups or socio-economic status. In the context of communication networks, the mobility may capture the movement of robots across sub-groups and different classes may capture the heterogeneity in robots.

The classic epidemic models consider well-mixed population (Hethcote, 2000). Network epidemic models relax the well-mixed assumption by considering interaction between sub-populations (Fall et al., 2007; Khanafer et al., 2016; Mei et al., 2017; Nowzari et al., 2016; Ogura and Preciado, 2016; Pagliara and Leonard, 2020; Paré et al., 2018). In these models, sub-populations are represented by nodes in the interaction graph and the infectious sub-population in neighboring nodes instantaneously influence the epidemic spread dynamics at a node.

In contrast, we focus on epidemic spread with mobility and use the class of models studied in (Jin and Wang, 2005; Li and Shuai, 2009; Wang and Zhao, 2004), wherein the interaction between neighboring nodes is due to the physical movement of individuals between them. In these works, the mobility or dispersal patterns depend on the state (susceptible or infected) of the individuals, and conditions for stability of equilibria are derived. These models have been extended in the context of SEIR models to capture the influence of multiple species (classes) in (Arino et al., 2005), wherein conditions for the global stability of a disease-free equilibrium are derived.

In this paper, we consider a patchy environment in which individuals within each patch may belong to different classes and their mobility across patches is determined by their class. This leads to a multi-layer mobility model and we study its interaction with SIR epidemic propagation. We extend the results for the deterministic network model (Abhishek and Srivastava, 2020; Fall et al., 2007; Khanafer et al., 2016; Mei et al., 2017) to the proposed model and characterize its steady state and stability properties.

The major contributions of this paper are threefold. First, we derive a deterministic continuum limit model describing the interaction of the SIR dynamics with the multi-layer Markovian mobility dynamics. The obtained model is similar to the model studied in (Arino et al., 2005); however, our presentation derives the model from first

⋆ This work was supported by ARO grant W911NF-18-1-0325.

principles. Second, we rigorously characterize the stability properties of the equilibrium point. Third, we provide some simple conditions for epidemic outbreak.

Mathematical notation: For any two real vectors $\boldsymbol{x}$, $\boldsymbol{y} \in \mathbb{R}^n$, we denote:
$\boldsymbol{x} \gg \boldsymbol{y}$, if $x_i > y_i$ for all $i \in \{1, \dots, n\}$,
$\boldsymbol{x} \geq \boldsymbol{y}$, if $x_i \geq y_i$ for all $i \in \{1, \dots, n\}$,
$\boldsymbol{x} > \boldsymbol{y}$, if $x_i \geq y_i$ for all $i \in \{1, \dots, n\}$ and $\boldsymbol{x} \neq \boldsymbol{y}$.
For any vector $\boldsymbol{x} = [x_1, \dots, x_n]^\top$, $X = \text{diag}(\boldsymbol{x})$ is a diagonal matrix with $X_{ii} = x_i$ for all $i \in \{1, \dots, n\}$.

2. SIR MODEL UNDER MULTI-LAYER MARKOVIAN MOBILITY

We consider n sub-populations of individuals that are located in distinct spatial regions (patches). We assume that the individuals within each patch can be classified into three categories: (i) susceptible, (ii) infected and (iii) recovered. Additionally, we assume that these individuals are further grouped into m classes depending on how they travel to other patches. Let the connectivity of these patches corresponding to the mobility pattern of each class $\alpha \in \{1, \dots, m\}$ be modeled by a digraph $\mathcal{G}^\alpha = (\mathcal{V}, \mathcal{E}^\alpha)$, where $\mathcal{V} = \{1, \dots, n\}$ is the node (patch) set and $\mathcal{E}^\alpha \subset \mathcal{V} \times \mathcal{V}$ is the edge set. We model the mobility of individuals on each graph $\mathcal{G}^\alpha$ using a Continuous Time Markov Chain (CTMC) with generator matrix Q^α, whose (i,j)-th entry is q_{ij}^α. The entry $q_{ij}^\alpha \geq 0$, $i \neq j$, is the instantaneous transition rate from node i to node j, and $-q_{ii}^\alpha = \nu_i^\alpha$ is the total rate of transition out of node i, i.e., $\nu_i^\alpha = \sum_{j \neq i} q_{ij}^\alpha$. Here, $q_{ij}^\alpha > 0$, if $(i,j) \in \mathcal{E}^\alpha$; and $q_{ij}^\alpha = 0$, otherwise. Let $x_i^\alpha(t)$ be the number of individuals of class α in patch i at time t. Let $p_i^\alpha \in [0,1]$ (respectively, $s_i^\alpha \in [0,1]$) be the fraction of infected (respectively, susceptible) individuals within individuals of class α at patch i. Define $\boldsymbol{p}^\alpha := [p_1^\alpha, \dots, p_n^\alpha]^\top$, $\boldsymbol{s}^\alpha := [s_1^\alpha, \dots, s_n^\alpha]^\top$, $\boldsymbol{x}^\alpha := [x_1^\alpha, \dots, x_n^\alpha]^\top$, $\boldsymbol{p} := [(\boldsymbol{p}^1)^\top, \dots, (\boldsymbol{p}^m)^\top]^\top$, $\boldsymbol{s} := [(\boldsymbol{s}^1)^\top, \dots, (\boldsymbol{s}^m)^\top]^\top$ and $\boldsymbol{x} := [(\boldsymbol{x}^1)^\top, \dots, (\boldsymbol{x}^m)^\top]^\top$.

For the epidemic process at node i, let $\beta_i > 0$ and $\delta_i \geq 0$ be the infection and recovery rate, respectively. We let $B^\alpha > 0$ and $D^\alpha \geq 0$ be the positive and non-negative diagonal matrices with entries β_i and δ_i, $i \in \{1, \dots, n\}$, respectively. Let B and D be the positive and non-negative diagonal matrices with block-diagonal entries B^α and D^α, $\alpha \in \{1, \dots, m\}$, respectively. Let $P^\alpha := \text{diag}(\boldsymbol{p}^\alpha)$, $P := \text{diag}(\boldsymbol{p})$ and $S := \text{diag}(\boldsymbol{s})$. We now derive the continuous time dynamics that captures the interaction of mobility and the SIR epidemic dynamics.

Proposition 1. (***SIR model under mobility***). The dynamic model for SIR epidemic process with multi-layer Markovian mobility is

$$\dot{\boldsymbol{s}} = -SBF(\boldsymbol{x})\boldsymbol{p} - L(\boldsymbol{x})\boldsymbol{s} \tag{1a}$$
$$\dot{\boldsymbol{p}} = (SBF(\boldsymbol{x}) - D - L(\boldsymbol{x}))\boldsymbol{p} \tag{1b}$$
$$\dot{\boldsymbol{x}}^\alpha = (Q^\alpha)^\top \boldsymbol{x}^\alpha, \tag{1c}$$

where L is an $nm \times nm$ block-diagonal matrix with block-diagonal terms L^α, $\alpha \in \{1, \dots, m\}$, $L^\alpha(\boldsymbol{x})$ is a matrix with entries

$$l_{ij}^\alpha(\boldsymbol{x}) = \begin{cases} \sum_{j \neq i} q_{ji}^\alpha \frac{x_j^\alpha}{x_i^\alpha}, & \text{if } i = j, \\ -q_{ji}^\alpha \frac{x_j^\alpha}{x_i^\alpha}, & \text{otherwise,} \end{cases}$$

$F(\boldsymbol{x}) := [\bar{F}^\top(\boldsymbol{x}), \dots, \bar{F}^\top(\boldsymbol{x})]^\top$ be a row-concatenated $nm \times nm$ matrix with each $n \times nm$ block-row as $\bar{F}(\boldsymbol{x}) := [F^1(\boldsymbol{x}), \dots, F^m(\boldsymbol{x})]$, and F^α as a diagonal matrix with entries $f_i^\alpha(\boldsymbol{x}) := \frac{x_i^\alpha}{\sum_\alpha x_i^\alpha}$, i.e., the fraction of total population at node i contributed by class α.

Proof: The proof follows similarly to that in (Abhishek and Srivastava, 2020, Proposition 1). □

We analyze the SIR model under multi-layer mobility (1) under the following standard assumptions:

Assumption 1. Digraph $\mathcal{G}^\alpha$ is strongly connected, for all $\alpha \in \{1, \dots, m\}$, which is equivalent to matrices Q^α being irreducible (Bullo (2020)). □

Assumption 2. There exists a node k such that $\delta_k > 0$. □

Let $\boldsymbol{v}^\alpha$ be the right eigenvector of $(Q^\alpha)^\top$ associated with eigenvalue at 0. We assume that $\boldsymbol{v}^\alpha$ is scaled such that its inner product with the associated left eigenvector $\boldsymbol{1}_n$ is unity, i.e., $\boldsymbol{1}_n^\top \boldsymbol{v}^\alpha = 1$. Define $\boldsymbol{v} := [N^1(\boldsymbol{v}^1)^\top, \dots, N^m(\boldsymbol{v}^m)^\top]^\top$, where N^α is the total number of individuals belonging to class α, for $\alpha \in \{1, \dots, m\}$.

Theorem 1. (***Existence and properties of equilibria***). For the SIR model with multi-layer Markovian mobility (1) under Assumptions 1 and 2, the following statements hold

(i) if $\boldsymbol{p}(0)$ and $\boldsymbol{s}(0) \in [0,1]^{nm}$, then $\boldsymbol{p}(t)$ and $\boldsymbol{s}(t) \in [0,1]^{nm}$ for all $t > 0$;
(ii) if $\boldsymbol{p}(0) > 0$ and $\boldsymbol{s}^\alpha(0) > 0$ for each α, then $\boldsymbol{p}(t) \gg 0$ and $\boldsymbol{s}(t) \gg 0$ for all $t > 0$;
(iii) the equilibrium points $(\boldsymbol{p}^*, \boldsymbol{s}^*, \boldsymbol{x}^*)$ belong to the set $\{(\boldsymbol{0}, [k_1 \boldsymbol{1}_n^\top, k_2 \boldsymbol{1}_n^\top, ..., k_m \boldsymbol{1}_n^\top]^\top, \boldsymbol{v}) \mid k_1, k_2, ..., k_m \in \mathbb{R}_{\geq 0}\}$;
(iv) the set of equilibria $\{(\boldsymbol{0}, [k_1 \boldsymbol{1}_n^\top, k_2 \boldsymbol{1}_n^\top, ..., k_m \boldsymbol{1}_n^\top]^\top, \boldsymbol{v}) \mid k_1, k_2, ..., k_m \in \mathbb{R}_{\geq 0}\}$ is globally asymptotically attractive.

Proof: (i) and (ii) follow similarly to the proof in (Abhishek and Srivastava, 2020, Theorem 1). Define $L^* := L(\boldsymbol{x}^*)$, $S^* := \text{diag}(\boldsymbol{s}^*)$ and $F^* := F(\boldsymbol{x}^*)$. To establish statement (iii), premultiply (1a) and (1b) with $\boldsymbol{x}^{*\top}$ at equilibrium

$$-\boldsymbol{x}^{*\top} S^* B F^* \boldsymbol{p}^* = 0 \tag{2a}$$
$$\boldsymbol{x}^{*\top} S^* B F^* \boldsymbol{p}^* - \boldsymbol{x}^{*\top} D \boldsymbol{p}^* = 0. \tag{2b}$$

Here, we have used the fact that $\boldsymbol{x}^{*\top} L^* = 0$, which can be seen from the fact that $\boldsymbol{x}^\top L(\boldsymbol{x}) = \boldsymbol{x}^\top Q$. Also, since $\boldsymbol{x}^* \gg \boldsymbol{0}$ and $S^* B F^* \boldsymbol{p}^* \geq \boldsymbol{0}, D\boldsymbol{p}^* \geq \boldsymbol{0}$, (2) yields

$$S^* B F^* \boldsymbol{p}^* = 0 \tag{3a}$$
$$D\boldsymbol{p}^* = 0. \tag{3b}$$

Using Assumption 2 in (3b) implies $p_k^{*\alpha} = 0$ for each α at node k with $\delta_k > 0$. Using (3) in (1b) at equilibrium gives $L^* \boldsymbol{p}^* = \boldsymbol{0}$ or equivalently $L^{*\alpha} \boldsymbol{p}^{*\alpha} = \boldsymbol{0}$ for each α. Therefore under strong connectivity assumption of each layer (Assumption 1) $\boldsymbol{p}^* = \boldsymbol{0}$. Further using (3a) in (1a) at equilibrium yields $L^* \boldsymbol{s}^* = \boldsymbol{0}$, or equivalently $L^{*\alpha} \boldsymbol{s}^{*\alpha} = \boldsymbol{0}$

which gives: $\boldsymbol{s}^{*\alpha} = k_\alpha \mathbf{1}_n$ for each α. This proves statement (iii).

For statement (iv), consider a Lyapunov candidate function $V_3 = \boldsymbol{x}^\top(2\boldsymbol{s} + \boldsymbol{p})$. It follows that

$$\begin{aligned}\dot{V}_3 &= \boldsymbol{x}^\top(-2SBF\boldsymbol{p} - 2L\boldsymbol{s} + SBF\boldsymbol{p} - D\boldsymbol{p} - L\boldsymbol{p}) \\ &\quad + \boldsymbol{x}^\top Q(2\boldsymbol{s} + \boldsymbol{p}) \\ &= \boldsymbol{x}^\top(-SBF\boldsymbol{p} - D\boldsymbol{p}) \\ &\leq 0.\end{aligned}$$

Now, using LaSalle's invariance theorem (Khalil, 2002, Theorem 4.4), all trajectory asymptotically goes to the largest invariant set with $\dot{V}_3 = 0$. This further implies all trajectory asymptotically goes to an invariant set with $D\boldsymbol{p} = 0$ and $SBF\boldsymbol{p} = 0$. Using this fact in (1b) at equilibrium expanded for each mobility layer under Assumptions 1 and 2 implies $\boldsymbol{p}^* = \mathbf{0}$ is globally attractive.

Next consider a Lyapunov candidate function $V_4 = \boldsymbol{s}^\top X^* \boldsymbol{s} - 2nmr \int_0^t (\|\tilde{L}\|)dt$ with $X^* := \mathrm{diag}(\boldsymbol{x}^*)$ and $r := \|X^*\|$. Then,

$$\begin{aligned}\dot{V}_4 &= 2\boldsymbol{s}^\top X^* \dot{\boldsymbol{s}} - 2nmr(\|\tilde{L}\|) \\ &= -2\boldsymbol{s}^\top X^* BFS\boldsymbol{p} + \boldsymbol{s}^\top(X^*(-L) + (-L)^\top X^*)\boldsymbol{s} \\ &\quad - 2nmr(\|\tilde{L}\|) \\ &= -2\boldsymbol{s}^\top X^* BFS\boldsymbol{p} - \boldsymbol{s}^\top(X^*(L^*) + (L^*)^\top X^*)\boldsymbol{s} \\ &\quad - \boldsymbol{s}^\top(X^*(\tilde{L}) + (\tilde{L})^\top X^*)\boldsymbol{s} - 2nmr(\|\tilde{L}\|) \\ &\leq -2\boldsymbol{s}^\top X^* BFS\boldsymbol{p} - \boldsymbol{s}^\top(X^*(L^*) + (L^*)^\top X^*)\boldsymbol{s} \\ &\quad + 2nmr(\|\tilde{L}\|) - 2nmr(\|\tilde{L}\|) \\ &\leq -2\boldsymbol{s}^\top X^* BFS\boldsymbol{p} - \boldsymbol{s}^\top(X^*(L^*) + (L^*)^\top X^*)\boldsymbol{s} \\ &\leq -\boldsymbol{s}^\top(X^*(L^*) + (L^*)^\top X^*)\boldsymbol{s} \leq 0.\end{aligned}$$

The last inequality follows as the matrix $X^*(L^*) + (L^*)^\top X^*$ is a symmetric Laplacian and hence a symmetric positive semi-definite matrix. To see this, note that $(X^*(L^*) + (L^*)^\top X^*)\mathbf{1} = X^*(L^*)\mathbf{1} + (L^*)^\top X^* \mathbf{1} = \mathbf{0} + (L^*)^\top \boldsymbol{x}^* = \mathbf{0}$. Additionally, this matrix is a block diagonal matrix with block elements as strongly connected symmetric Laplacian matrices. Using Barbalat's lemma, we get $\dot{V}_4 \to 0$. This in turn leads to $\boldsymbol{s} \to [k_1\mathbf{1}_n^\top, k_2\mathbf{1}_n^\top, \ldots, k_m\mathbf{1}_n^\top]^\top$. This proves statement (iv). □

An epidemic outbreak is an event in which the total number of infected individuals in the system (summed over all the layers and nodes) increase before eventually reaching a disease-free state. As evident from Theorem 1, the total number of infected individuals ultimately goes to zero. The epidemic outbreak is characterized by the increase in the size of the infected population in the early phase of the transient response.

Define $s_{\max}(t)$ as the greatest element in $\boldsymbol{s}(t)$ taken over all layers and nodes.

Corollary 1. (***Epidemic outbreak***). For the SIR epidemic model under multi-layer Markovian mobility (1) under Assumption 1, the following statements hold

(i) For a single layer network, if $s_{\max}(0)B - D \leq 0$ then there is no epidemic outbreak and total infected population monotonically decreases to zero;
(ii) If $S(0)BF(0) - D > 0$, then there is an epidemic outbreak at $t = 0$.

Proof: Using (1b), we first write the expression for the rate of change of total infected population for the system, $N_I = \boldsymbol{x}^\top \boldsymbol{p}$:

$$\begin{aligned}\dot{N}_I &= \boldsymbol{x}^\top \dot{\boldsymbol{p}} + \dot{\boldsymbol{x}}^\top \boldsymbol{p} \\ &= \boldsymbol{x}^\top(SBF(\boldsymbol{x}) - D - L(\boldsymbol{x}))\boldsymbol{p} + \boldsymbol{x}^\top Q\boldsymbol{p} \\ &= \boldsymbol{x}^\top(SBF(\boldsymbol{x}) - D)\boldsymbol{p} \qquad (4)\end{aligned}$$

where (4) follows using $\boldsymbol{x}^\top L(\boldsymbol{x}) = \boldsymbol{x}^\top Q$, a consequence of definitions of matrices $L(\boldsymbol{x})$ and Q. It can be shown from (1a) that $s_{\max}(t)$ monotonically decreases with time. This is a consequence of negative first term and negative Laplacian second term in the right hand side of (1a). Now, for the special case of a single layer network $F(\boldsymbol{x}) = I$, therefore in the right hand side of (4), we can see that $SB - D \leq s_{\max}(t)B - D \leq s_{\max}(0)B - D$. Further, since $\boldsymbol{x}$ and $\boldsymbol{p}$ are non-negative, if $s_{\max}(0)B - D \leq 0$, then for a single layer network the right hand side of (4) is non-positive and hence N_I monotonically decreases. This proves statement (i).

Statement (ii) follows by evaluating $SBF - D$ at $t = 0$ and making it positive to make right side of (4) positive at $t = 0$ and hence N_I increases at $t = 0$ giving rise to an initial outbreak. □

3. NUMERICAL ILLUSTRATIONS

In this section, we numerically illustrate our results on multi-layer SIR epidemic model.

We choose different population size for the two mobility layers and select the mobility transition rates using the Metropolis-Hastings algorithm (Hastings, 1970) such that the equilibrium distribution of population is the same for both the layers (taken as uniform equilibrium distribution).

Figures 1 (a) and (b) show the fractions of infected population whereas Figures 1 (c) and (d) show the fraction of susceptible population trajectories for 10 nodes connected with 2-layers of graph structures. Layer 1 is line graph and layer 2 is ring graph. The initial population distribution at the 10 nodes for layer 1 and layer 2 are

$5 \times [700, 500, 300, 100, 500, 700, 800, 900, 600, 500]$, and
$5 \times [300, 300, 200, 100, 200, 300, 400, 400, 500, 200]$,

respectively. The infection and curing rates for the 10 nodes are

$[0.31, 0.32, 0.35, 0.36, 0.5, 0.3, 0.3, 0.1, 0.1, 0.1]$, and
$[0.3, 0.22, 0.21, 0.25, 0.3, 0.21, 0.23, 0.24, 0.21, 0.22]$,

respectively. The initial fraction of infected population is taken as 0.01 for all layers and nodes with no recovered population.

4. CONCLUSIONS

We derived a continuous-time model for SIR epidemic propagation under Markovian mobility across multi-layer network of patches. The derived model has been analysed to establish properties of the equilibria. Some simple conditions for epidemic outbreak have been established. We also provided numerical studies to support our results. The work can be extended to do further analyses, for example, analysis of transient dynamics for the presence

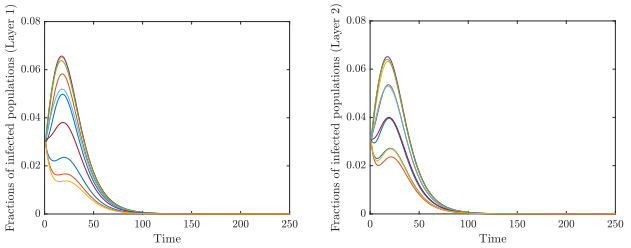

(a) Infected population; graph 1 (b) Infected population; graph 2

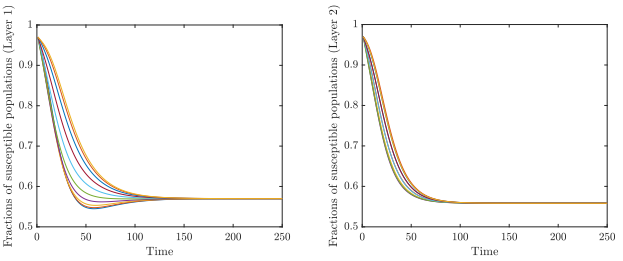

(c) Susceptible population; graph 1 (d) Susceptible population; graph 2

Fig. 1. Simulation of deterministic model of SIR epidemic spread under 2 layer mobility, over Line-Ring graph structure. $n = 10$, $p_i(0) = 0.01$.

of outbreaks as well as to study the effect of network structure on the transient dynamics.

REFERENCES

Abhishek, V. and Srivastava, V. (2020). SIS epidemic model under mobility on multi-layer networks. In *American Control Conference*, 3743–3748. Denver, CO.

Arino, J., Davis, J.R., Hartley, D., Jordan, R., Miller, J.M., and Van Den Driessche, P. (2005). A multi-species epidemic model with spatial dynamics. *Mathematical Medicine and Biology*, 22(2), 129–142.

Bullo, F. (2020). *Lectures on Network Systems*. Kindle Direct Publishing, 1.4 edition. URL `http://motion.me.ucsb.edu/book-lns`. With contributions by J. Cortes, F. Dorfler, and S. Martinez.

Calafiore, G.C., Novara, C., and Possieri, C. (2020). A modified SIR model for the COVID-19 contagion in italy. *arXiv preprint arXiv:2003.14391*.

Fall, A., Iggidr, A., Sallet, G., and Tewa, J.J. (2007). Epidemiological models and Lyapunov functions. *Mathematical Modelling of Natural Phenomena*, 2(1), 62–83.

Franco, E. (2020). A feedback SIR (fSIR) model highlights advantages and limitations of infection-based social distancing. *arXiv preprint arXiv:2004.13216v1*.

Hastings, W.K. (1970). Monte carlo sampling methods using Markov chains and their applications. *Biometrika*, 57(1), 97–109.

Hethcote, H.W. (2000). The mathematics of infectious diseases. *SIAM Review*, 42(4), 599–653.

Jin, F., Dougherty, E., Saraf, P., Cao, Y., and Ramakrishnan, N. (2013). Epidemiological modeling of news and rumors on twitter. In *Workshop on Social Network Mining and Analysis*, 1–9.

Jin, Y. and Wang, W. (2005). The effect of population dispersal on the spread of a disease. *Journal of Mathematical Analysis and Applications*, 308(1), 343–364.

Khalil, H.K. (2002). *Nonlinear Systems*. Prentice Hall, third edition.

Khanafer, A., Başar, T., and Gharesifard, B. (2016). Stability of epidemic models over directed graphs: A positive systems approach. *Automatica*, 74, 126–134.

Kleinberg, J. (2007). The wireless epidemic. *Nature*, 449(7160), 287.

Li, M.Y. and Shuai, Z. (2009). Global stability of an epidemic model in a patchy environment. *Canadian Applied Mathematics Quarterly*, 17(1), 175–187.

Mei, W., Mohagheghi, S., Zampieri, S., and Bullo, F. (2017). On the dynamics of deterministic epidemic propagation over networks. *Annual Reviews in Control*, 44, 116–128.

Morris, D.H., Rossine, F.W., Plotkin, J.B., and Levin, S.A. (2020). Optimal, near-optimal, and robust epidemic control. *arXiv preprint arXiv:2004.02209*.

Nowzari, C., Preciado, V.M., and Pappas, G.J. (2016). Analysis and control of epidemics: A survey of spreading processes on complex networks. *IEEE Control Systems Magazine*, 36(1), 26–46.

Ogura, M. and Preciado, V.M. (2016). Stability of spreading processes over time-varying large-scale networks. *IEEE Transactions on Network Science and Engineering*, 3(1), 44–57.

Pagliara, R. and Leonard, N.E. (2020). Adaptive susceptibility and heterogeneity in contagion models on networks. *IEEE Transactions on Automatic Control*, 1–1.

Paré, P.E., Beck, C.L., and Nedić, A. (2018). Epidemic processes over time-varying networks. *IEEE Transactions on Control of Network Systems*, 5(3), 1322–1334.

Wang, P., González, M.C., Hidalgo, C.A., and Barabási, A.L. (2009). Understanding the spreading patterns of mobile phone viruses. *Science*, 324(5930), 1071–1076.

Wang, W. and Zhao, X.Q. (2004). An epidemic model in a patchy environment. *Mathematical Biosciences*, 190(1), 97–112.

Zhang, X., Neglia, G., Kurose, J., and Towsley, D. (2007). Performance modeling of epidemic routing. *Computer Networks*, 51(10), 2867–2891.